JOURNAL OF MATERIALS SCIENCE 32 (1997) 5413–5417

Carbide formation in aluminium–carbon fibre-reinforced composites

H.-D. STEFFENS, B. REZNIK, V. KRUZHANOV
Institute of Materials Engineering, University of Dortmund, Germany
W. DUDZINSKI
Institute of Materials Science and Applied Mechanics, Technical University of Wrocław, Poland

New results on the carbide formation in aluminium–carbon fibre composites are reviewed, with their implications for technology, including vacuum infiltration of carbon-fibre preforms with liquid aluminium. The microstructure of infiltrated specimens was studied with the aid of transmission electron microscopy. Most lath-like carbide crystals investigated in this work are twins. Twinning is probably connected with the squeezing stresses during matrix cooling due to a high difference in thermal expansion coefficients of carbide and metal. The analytical description of experimental data in the light of the crystal-growth concept allows us to conclude that carbides grow during infiltration, predominantly at the time of fibre contact with molten aluminium, but not during matrix solidification and its subsequent cooling. The growth rate of carbide crystals is limited rather by the interface kinetics than by carbon diffusion in the melt as was assumed previously. This allows some effective methods of process control to be found, for example, growth step retardation by means of an adsorption-active impurity.

1. Introduction

During the processing of aluminium–carbon fibre-reinforced composites, aluminium carbide formation takes place at the interface between the aluminium matrix and the fibre. The presence of carbide particles may strongly influence the mechanical properties of the composite (e.g. [1]). In this connection, essential information is likely to be obtained by investigating the peculiarities of the carbide formation with the aim of finding possibilities for a production-process control.

Carbide formation takes place in various processing technologies for composites, in particular during vacuum infiltration of carbon fibres with liquid aluminium. The structure of composites produced by this method has been studied carefully. Some basic results were described in recent papers [2–5]. It was shown that carbides may grow at the fibre surface, forming lath-like crystals of rhombohedral structure with (0 0 0 1) basal planes. The longitudinal axes of these crystals are closely parallel to the $[1\,1\,\bar{2}\,0]$ crystallographic direction.

The obtained data occasionally may be connected with limited comparability caused by different processing methods and parameters (temperature, pressure and time) as well as different kinds of initial materials (fibres and matrix alloys). Sometimes chemically developed carbon fibres and aluminium matrices containing different alloying components are used. For this purpose it was regarded advantageous to study the described process in the most simple case of non-developed carbon fibre and pure aluminium matrix by using transmission electron microscopy. Moreover, in the literature there is no clear understanding of factors that limit the process of carbide growth. Therefore, an attempt has been made to describe analytically the growth of carbide crystals based on experimental investigations of structure formation.

2. Experimental procedure

The composite material investigated in this work was produced by "Aluminium Ranshofen GmbH" (Austria) by gas pressure infiltration [6]. Preform of high-strength fibres EXAS-6k2 ($E = 230$ GPa, UTS $= 4000$ MPa, mean diameter 6.8 μm, manufactured by Courtaulds Aerospace Ltd, Coventry) was held at 700 °C before infiltration.

Owing to the higher reactivity of low-oriented high-strength fibres (with respect to highly oriented high-modulus fibres [7]), the contact time between liquid metal and fibres was minimized. The gas pressure infiltration with the melt of commercially pure aluminium (Al 99.85%) took place during 3 min at a temperature of 730 °C.

Specimens for transmission electron microscopy, sections approximately 0.1 mm thick, were cut perpendicular to the fibre axis. The sections were removed as

3 mm discs which were dimpled mechanically and polished with diamond paste in a Gatan Dimpler Grinder to a central thickness of 15 μm. Final perforation to electron transparency was carried out by argon-ion sputtering in a Duo Mill apparatus. The conditions for ion milling were 8 kV at 10° gun tilt until penetration and then 4 kV at 4° gun tilt to remove the damaged layer produced by higher voltage milling. The specimens were examined in a Jeol-2000-FX transmission electron microscope operated at 200 kV.

3. Results and discussion

Fig. 1 shows the infiltrated specimen at a low magnification. It can be seen that the carbon fibres are distributed homogeneously and that there is no visible porosity. This confirms that the vacuum infiltration process finished by the complete filling of the preform volume. The studies at higher magnifications have revealed the presence of precipitates in the interface area between fibre and matrix (Fig. 2). Selected-area diffraction analysis (SAD) has shown that these precipitates are of Al_4C_3 type with a rhombohedral structure and (0 0 0 1) basal planes. They have lath-like form and are elongated with [1 1 $\bar{2}$ 0]-axis orientation which is in agreement with results of previous investigations [3–5].

As was found previously [3, 4], the nucleation of carbide crystals occurred predominantly at the carbon-fibre surface (Fig. 3). Carbide crystals grow more rapidly along the [1 1 $\bar{2}$ 0] direction showing clearly visible faceted shape and step-like growth morphology (Fig. 2). This allows us to conclude that crystal growth occurs by means of a ledge-movement mechanism and not by so-called normal growth [8]. The carbon surface microstructure is rather turbostratic than well-developed (Figs 3, 4). That is why no clear evidence of any kind of epitaxy can be observed between carbide and carbon fibre surface. Nevertheless, as was found elsewhere [3, 4], the nucleation of carbide crystals occurred predominantly at the carbon-fibre surface (Fig. 3) near the source of carbon.

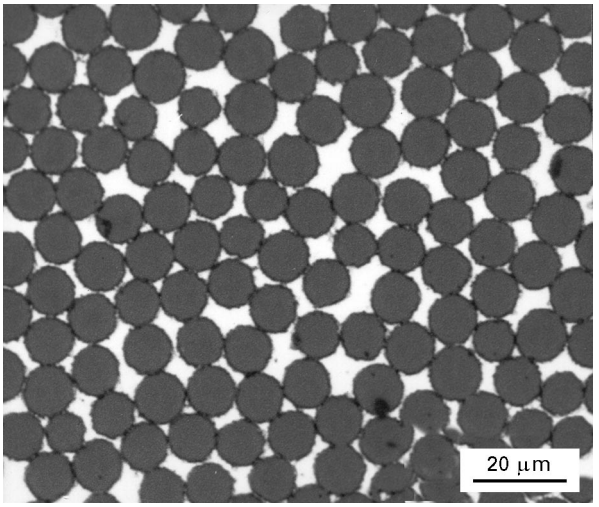

Figure 1 A cross-section of infiltrated Al/C composite.

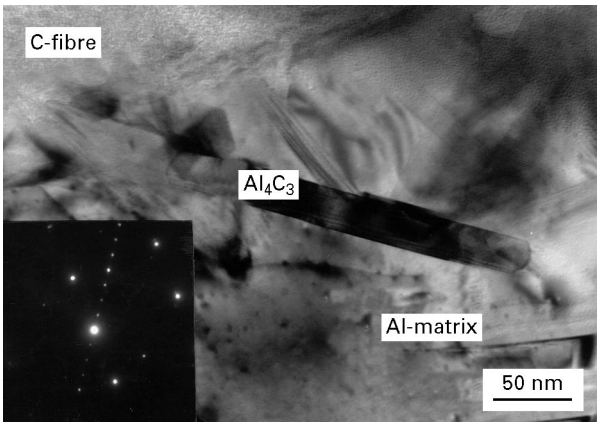

Figure 2 Interface area between the carbon fibre and the aluminium matrix and SAD-pattern of Al_4C_3 and aluminium.

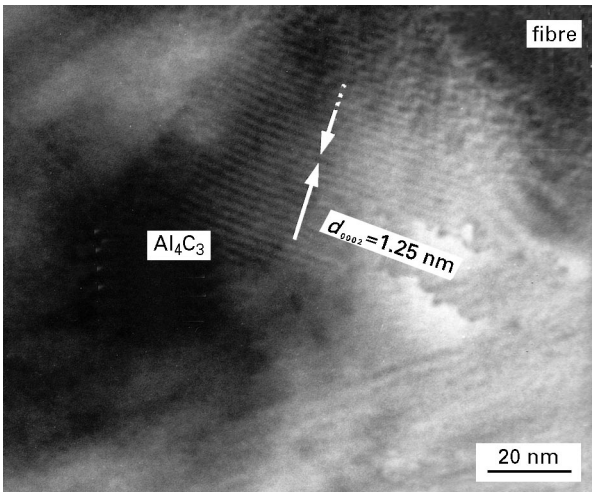

Figure 3 Microstructure of the contact area between the carbon fibre and aluminium carbide.

For a better understanding of carbide formation in composites, it is essential to elucidate the conditions of its growth: either it takes place exclusively during the infiltration, when carbon fibre is in contact with the liquid metal, or also during and after solidification of the matrix [1]. It was shown by Yang and Scott [3], that the thermal treatment at temperatures near the aluminium melting point that follows infiltration has no effect on the structure and quantity of carbide precipitates. Thus, carbides may be formed when the fibre comes into contact with liquid aluminium, or during the solidification of the matrix.

The growth of carbide crystals in liquid aluminium may be described as a three-stage process: (1) dissolution of carbon fibre in liquid aluminium; (2) carbon diffusion, producing a homogeneous distribution in the melt and its transport to the growing carbide surface; (3) deposition of carbon atoms in moving growth steps of the carbide crystal surface.

The first stage of the process immediately begins at the very moment of fibre contact with liquid aluminium. The dissolution flux is proportional to the difference between the equilibrium carbon concentration in liquid aluminium near the carbon fibre surface, C_f^0,

and the actual carbon concentration in the melt, C

$$j_\alpha = \alpha(C_f^0 - C) \tag{1}$$

where j_α is a dissolution flux ($cm^{-2}s^{-1}$) and α is the kinetic coefficient of dissolution ($cm\,s^{-1}$). The amount of carbon atoms, n, which are dissolved from the surface, s, in volume, v, gives the carbon concentration $C = n/v$. The rate of variation in concentration can be described by the following differential equation

$$\frac{dC}{dt} = \alpha \frac{s}{v}(C_f^0 - C) \tag{2}$$

The solution of this equation under the initial condition $C = 0$ at $t = 0$ is

$$C = C_f^0\left[1 - \exp\left(-\alpha \frac{s}{v} t\right)\right] \tag{3}$$

which can be written as

$$t = -\frac{1}{\alpha}\frac{v}{s}\ln\left(1 - \frac{C}{C_f^0}\right) \tag{4}$$

The time at which concentration close to the saturation is established, can be estimated. In the ideal case of close hexagonal packing of fibres, it is easy to show that the volume of the intervening space between three fibres of the radius r and unit length is $v = r^2(3^{1/2} - \pi/2)$, and the surface enclosing this volume is $s = \pi r$. The relationship of volume to surface is

$$\frac{v}{s} = \left(\frac{3^{1/2}}{\pi} - \frac{1}{2}\right)r \simeq \frac{r}{20} \tag{5}$$

Although the value of this relationship is actually larger, it can be used for a rough estimation. There are no data in the literature about the dissolution kinetic coefficient of carbon in liquid aluminium, but considering the dissolution symmetrically to the crystal growth one can use a characteristic value of the kinetic coefficient for crystal growth, which can be changed in relatively wide limits (10^{-3}–10^{-1}) $cm\,s^{-1}$ [8]. Using α in this interval and $r = 3.4$ μm, the maximum time, t, necessary for establishing the concentration $C = 0.99\,C_f^0$, is found to $t \approx 10^{-1}$ s, which is negligible in relation to the time of infiltration. Consequently, the carbide growth is not limited by carbon dissolution.

During the second stage, a homogeneous distribution of carbon in the melt occurs by diffusion. The characteristic time for establishment of a homogeneous distribution can be evaluated as

$$\tau \approx \frac{x^2}{D} \tag{6}$$

where x is the characteristic size of the intervening space between fibres and D is the diffusion coefficient of carbon in liquid aluminium. In the case of close packing of fibres, $x = r(3^{1/2} - 1)/2$. In a first approximation, the value of x can be taken as $x \approx 10^{-4}$ cm. A typical value for a diffusion coefficient in liquids is about 10^{-5} cm^2/s^{-1}. Using these values of x and D we have $\tau \approx 10^{-3}$ s, which is smaller than the time necessary for the saturation of the melt with carbon.

To consider the growth of a solitary carbide crystal in the case where it is relatively distant from other crystals, the distances between the crystals should be significantly larger than their sizes. In this case, the crystal grows and reduces the carbon concentration in the melt near the carbide surface to some value of C_c which is larger than its equilibrium value, C_c^0.

Taking the crystal in a cylindrical form with a radius R, the carbon concentration in the melt approaches the value of C_f^0 in a distance of the order of R from the growing surface. The concentration gradient, ∇C, that initiates the diffusion flow to the growing surface can be evaluated as $\nabla C \approx (C_f^0 - C_c)/R$ with the diffusion flow

$$j_D \approx \frac{D(C_f^0 - C_c)}{R} \tag{7}$$

The flow of atoms constituting growth steps is proportional to the difference between C_c and C_c^0 and is determined as [8]

$$j_\beta = \beta(C_c - C_c^0) \tag{8}$$

where β is a growth kinetic coefficient. Setting the flow of transport (Equation 7) at the interface equal to the flow of deposition (Equation 8)

$$C_c \approx \left(C_f^0 + \frac{\beta R}{D} C_c^0\right)\Big/\left(1 + \frac{\beta R}{D}\right) \tag{9}$$

Taking into account that the crystal growth rate is equal to

$$V = \frac{1}{3}\omega j_\beta \tag{10}$$

(ω is the volume of carbide molecule in the solid state; 1/3 is a coefficient, considering the carbide molecule to have three atoms of carbon), and substituting Equations 8 and 9 into 10, we obtain

$$V \approx (\beta\omega(C_f^0 - C_c^0))\Big/\left[3\left(1 + \frac{\beta R}{D}\right)\right] \tag{11}$$

As can be seen from Equation 11, the character of crystal growth is determined by the value of the second term in the denominator. With $\beta R/D \gg 1$ the growth is completely limited by carbon diffusion in the melt and is independent of the kinetics of surface processes. In this case (diffusion kinetics), the growth rate will be

$$V \approx \frac{D\omega}{3R}(C_f^0 - C_c^0) \tag{12}$$

In the case of $\beta R/D \ll 1$ (interface kinetics), the growth rate is determined by the interface kinetic processes and is

$$V \approx \frac{\beta\omega}{3}(C_f^0 - C_c^0) \tag{13}$$

Unfortunately, there are no data available in the literature about the growth kinetic coefficient of Al_4C_3. According to Chernov [8], the characteristic values of β are about (10^{-3}–10^{-1}) $cm\,s^{-1}$. By the growth of such fine disperse crystals (a cross-section

is not bigger than 50 nm), assuming that $D \approx 10^{-5}\ \mathrm{cm^2\,s^{-1}}$, the inequality $\beta R/D \ll 1$ is fulfilled with a large margin for all β in the mentioned limits. Consequently, the growth of carbides is limited by the interface kinetics, but not by diffusion as was assumed recently [3].

There is a basic meaning in the conclusion that the growth of carbides is limited by the interface kinetics which, as a consequence might provide for possibilities to influence the process of carbide formation. In the case of diffusion kinetics, there is only a little chance to influence significantly the diffusivity in a liquid, and consequently the crystal growth. In an opposite case, when the crystal growth is limited by step movement, it is possible to control this process, for example by means of inserting a small amount of adsorption-active impurities into the melt [8].

On the basis of experimental data indicating an average carbide size of about 0.5 μm after 3 min infiltration time, it is possible to estimate the value of β from Equation 12. The value of ω for Al_4C_3 is equal to $8 \times 10^{-23}\ \mathrm{cm^3}$. According to Dorward [9], the equilibrium concentration of carbon in liquid aluminium at a temperature of about 700 °C is 10^{-3} wt% or $C_f^0 \approx 1.2 \times 10^{18}\ \mathrm{cm^{-3}}$. The value of C_c^0 is expected to be negligible in relation to C_f^0, as the chemical reaction $4Al + 3C \rightleftarrows Al_4C_3$ will predominantly run in the direction of carbide formation under the given conditions. Thus a reasonable value of $\beta \approx 10^{-2}\ \mathrm{cm\,s^{-1}}$ can be obtained from Equation 13.

As the solubility of carbon in a solid phase is significantly lower than in a liquid during the time of matrix solidification, the aluminium melt must be supersaturated with carbon if carbides should be formed. In this particular case, the specific volume of carbides can be estimated as $7/3(C^l - C^s)$, where C^l and C^s are the equilibrium carbon concentrations (in at %) in liquid and solid aluminium, respectively. The factor 7/3 is connected with the chemical formula of Al_4C_3. For the system ($C^l - C_f^0 \cong 2 \times 10^{-3}$ at % [9]) and with the limits of $C^s \ll C^l$, the estimation gives a value of 5×10^{-5}. It is obvious that the actual concentration should be significantly higher than the obtained value. This shows that the carbide formation will predominantly occur at the time of fibre contact with liquid aluminium.

It should be pointed out that, as a significant feature of investigated Al_4C_3 crystals, twin formation is frequently observed (Fig. 4). The presence of twins in Al_4C_3 was first found here and is not yet clear in detail, but some comments may be made. As can be seen from Fig. 5a, Al_4C_3 crystals consist of single-twinning packets having a cross-section of about 10 nm and angle of approximately 55° between the packets. A twinning structure makes itself evident also in additional electron diffraction reflexes. The graphical interpretation of electron diffraction patterns, shown in Fig. 5b, illustrates the origination of extra spots due to microtwinning.

Taking into account that the ratio of lattice parameters c/a of Al_4C_3 is large ($c/a = 7.505$), it may be concluded the most likely mode of twinning is shear parallel to the basal planes [10]. Using formal crystallographic description given in terms of deformation twinning theory for hexagonal closed-packed crystals [11], twinning in Al_4C_3 parallel to (0 0 0 1) plane in the [1 1 $\bar{2}$ 0] direction is most likely to occur.

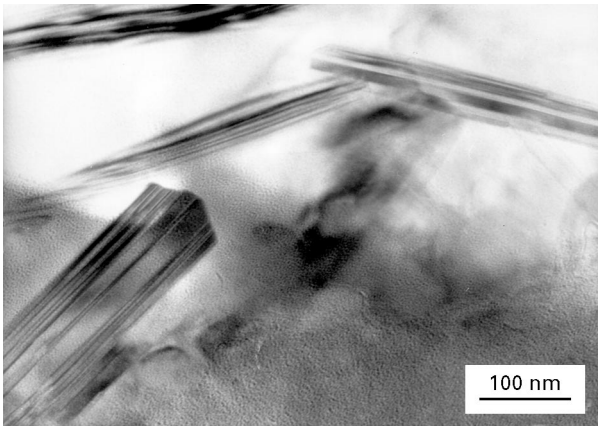

Figure 4 Twin crystals of aluminium carbide.

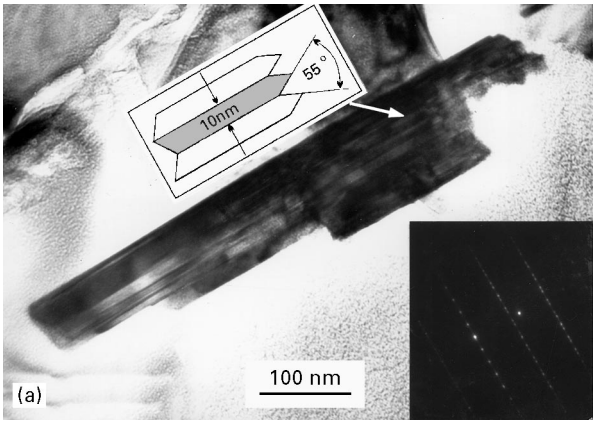

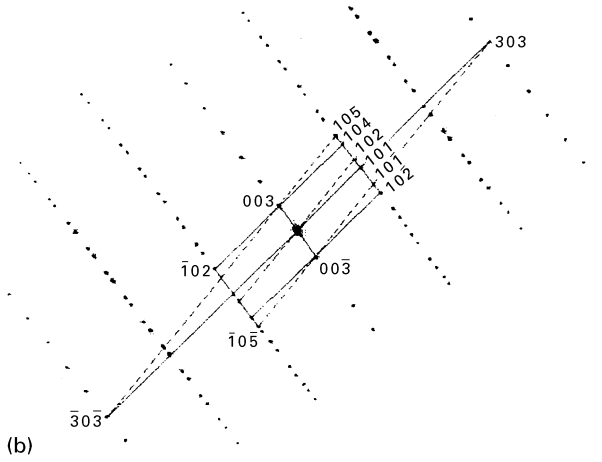

Figure 5 (a) Morphology of a twinned carbide crystal, and (b) interpretation of the corresponding SAD-pattern.

As well known, twins may usually originate during crystal growth or crystal deformation [11]. In this case, the deformation nature is supported by the fact that, after matrix solidification during cooling to room temperature, carbide crystals are under compressive strain due to a high difference in the thermal expansion coefficients of carbide and metal (3.6×10^{-6} and 2.5×10^{-5}

K^{-1}, respectively [12]). Those stresses may probably be the reason for twin formation. Further studies of twin formation of Al_4C_3 crystals can be of interest in connection with their part in mechanical binding between fibre and matrix.

4. Conclusions

1. During the production process of Al–C composites by means of infiltration, carbides will grow predominantly at the time of fibre contact with liquid aluminium but not during matrix solidification and subsequent cooling.

2. The growth rate of carbide crystals is limited by the interface kinetics rather than by the carbon diffusion into the melt. This allows effective methods of process control to be found; for example, growth step retardation by means of active-impurity adsorption.

3. Most lath-like carbide crystals investigated in this work are twins, which is probably connected with the squeezing stresses during matrix cooling.

Acknowledgements

The authors thank Dr J. Janczak, EMPA, Thun, Switzerland, for the provision of samples for investigation, and Professor H. P. Degischer, Leichtmetall-Kompetenzzentrum Ranshofen, Austria, for helpful discussions.

References

1. H. P. DEGISCHER, P. SCHULZ, W. LACOM and J. LANGGARTNER, in "*Proceedings of 3rd International Symposium on Structural and Functional Gradient Materials*", Lausanne, 1994, edited by B. Ilschner and R. Cherradi (EPFL, Lausanne, 1994) p. 30.
2. M. YANG and V. D. SCOTT, *J. Mater. Sci.* **26** (1991) 1609.
3. *Idem*, *Carbon* **29** (1991) 877.
4. A. P. DIWANJI and I. W. HALL, *J. Mater. Sci.* **27** (1992) 2093.
5. M. De SANCTIS, S. PELLETIER, Y. BIENVENU and M. GUIGON, *Carbon* **32** (1994) 925.
6. P. DEGISCHER, in "*Proceedings of the Conference* "*Verbundwerkstoffe und Werkstoffverbunde*", Bayreuth, October, 1995, edited by G. Ziegler (DGM, Oberusel, 1995) p. 139.
7. S. KOHARA and N. MUTO, *International Conference on Composite Materials V* ", San Diego, 1985, edited by W. C. Harrigan Jr, F. R. Strife and A. K. Dhingra (AIME TMS Publications, Warrendale, USA, 1985) p. 631.
8. A. A. CHERNOV, "Modern Crystallography III" (Springer, Berlin, 1984).
9. R. C. DORWARD, in "*Light Metals*", *Proceedings of the AIME Annual Meeting*, edited by A. V. Clack (AIME, New York, 1973) **102** (1) p. 105.
10. R. W. CAHN (ed.), "Physical metallurgy" (North Holland, Amsterdam 1970).
11. L. A. SHUVALOV (ed.), "Modern Crystallography IV" (Springer, Berlin, 1988).
12. H. NAYEB-HASHEMI and J. SEYYEDI, *Metall. Trans.*, **20A** (1989) 727.

Received 19 April 1996
and accepted 18 April 1997